Main, P., Fiske, S. J., Hull, S. E., Lessinger, L., Germain, G., Declercq, J.-P. & Woolfson, M. M. (1982). *MULTAN11/82. A System of Computer Programs for the Automatic Solution of Crystal Structures from X-ray Diffraction Data.* Univs. de York, Angleterre, et de Louvain, Belgique.

Scott, B. A., Giess, E. A. & O'Kane, D. F. (1969). *Mater. Res. Bull.* **4**, 107–117.

Stout, G. & Jensen, L. H. (1968). Dans *X-ray Structure Determination.* Londres: MacMillan.

Van Uitert, L. G., Levinstein, H. J., Rubin, J. J., Capio, C. D., Dearborn, E. F. & Bonner, W. A. (1968). *Mater. Res. Bull.* **3**, 47–57.

Van Uitert, L. G., Singh, S., Levinstein, H. J., Geusic, J. E. & Bonner, W. A. (1967). *Appl. Phys. Lett.* **11**, 161–163.

Walker, N. & Stuart, D. (1983). *Acta Cryst.* A**39**, 158–166.

$Fe_2Al_3Si_3$

C. GUENEAU AND C. SERVANT

Laboratoire de Métallurgie Structurale, URA CNRS 1107, Université Paris Sud, 91405 Orsay CEDEX, France

F. D'YVOIRE

Laboratoire de Chimie des Solides, URA CNRS 446, Université Paris Sud, 91405 Orsay CEDEX, France

N. RODIER

Laboratoire de Chimie Minérale, Faculté des Sciences Pharmaceutiques et Biologiques, 5 rue J.-B. Clément, 92296 Châtenay-Malabry CEDEX, France

Abstract

The structure of diiron trialuminium trisilicide is a compact three-dimensional arrangement of three symmetry-non-equivalent FeM_{10} and one FeM_9 Fe-centred polyhedra (M = Al or Si) connected by face, edge and corner sharing. The average distances are Fe—Si 2.381 and Fe—Al 2.585 Å. Si has 9–11 neighbours and Al 11 or 12 neighbours at distances less than 3.1 Å.

Comment

Industrial ferrosilicon alloys containing about 65 wt% Si have several applications in foundry and steel metallurgy, notably as cast-iron inoculants (graphite nucleation agents) and for the elaboration of thin magnetic sheets. They contain two major phases: an α-leboite ($FeSi_{2.4}$) matrix and pure silicon in the form of platelets. A few percent of alloying elements such as Al, Ca, Mn and Zr enter the composition of some minor phases. The effects of these elements on the grinding behaviour of the material have been investigated (Guéneau, 1993). In model ferrosilicon alloys containing 1–4 wt% Al, two phases of nominal formulae $FeAl_3Si_2$ and $Fe_2Al_3Si_3$ were observed. The crystal structure of $FeAl_3Si_2$ is reported elsewhere (Guéneau, Servant, d'Yvoire & Rodier, 1995). The compound $Fe_2Al_3Si_3$ was discovered by Zarechnyuk, German, Yanson, Rykhal & Muraveva (1981) who refer to it as $Al_{40}Fe_{22}Si_{38}$. Anglézio (1990) observed its presence in industrial ferrosilicon alloys and used the formula $Fe_5Al_8Si_7$. The formula $Fe_2Al_3Si_3$ adopted here is in closer agreement with the crystal structure, but is idealized. Our electron microprobe analyses indicate a composition range with the following atomic percentages: Fe 22.7–25, Al 38.5–42, Si 33–37.5% (calculated for $Fe_2Al_3Si_3$: 25, 37.5 and 37.5%, respectively). The composition of the crystal investigated closely fits the formula $Fe_2Al_{3.2}Si_{2.8}$, which suggests a partial substitution of Al for Si.

The structure is a compact arrangement of FeM_{10} and FeM_9 polyhedra (M = Al or Si) connected by face, edge and corner sharing. Fig. 1(a) represents what can be considered as the basic unit of the structure, *i.e.* four polyhedra, $Fe(1)M_{10}$, $Fe(2)M_{10}$, $Fe(3)M_{10}$ and $Fe(4)M_9$, hereafter designated by [Fe1], [Fe2], [Fe3] and [Fe4], respectively, centred on Fe atoms lying on the same (010) plane. [Fe1] and [Fe2] share a rectangular face, Si(3)–Al(6)–Si(4)–Al(6) (see Table 2), with a relatively short Fe(1)—Fe(2) distance (2.816 Å). [Fe1] and [Fe3] share an edge, as do [Fe2] and [Fe4]. As shown in Fig. 1(b), such basic units are linked by a common edge, Al(1)–Al(2), to form infinite strips running parallel to [100]. The strips lying on the same (010) plane are isolated from one another but are connected by corner (*C*), edge (*E*) or face (*F*) sharing with the strips lying on adjacent layers. The connections between polyhedra are listed in Table 3.

Another description of the structure can be given in terms of the alternate stacking of corrugated layers *A* and *B* parallel to (001) (Fig. 1b). In the *A* layer, which contains [Fe1] and [Fe2] polyhedra, each [Fe1] (or [Fe2]) polyhedron is connected to four [Fe2] ([Fe1]) polyhedra by face or edge sharing. In the *B* layer, comprising [Fe3] and [Fe4] polyhedra, each [Fe3] ([Fe4]) polyhedron is connected to two [Fe3] ([Fe4]) and four [Fe4] ([Fe3]) polyhedra by edge sharing. In addition, adjacent *A* and *B* layers have faces, edges and corners in common.

The interatomic distances (Table 2) agree satisfactorily with the values observed in other intermetallic compounds. As expected, the Si—Fe distances (mean value 2.381 Å) are significantly shorter than the Al—Fe distances (mean value 2.585 Å). The slightly longer Si(1)—Fe and Si(6)—Fe mean distances, compared with
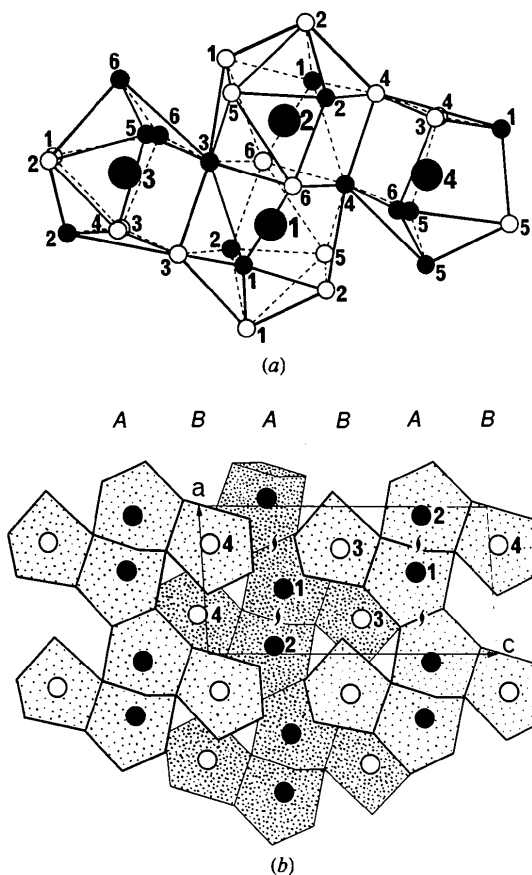
(a)

A　B　A　B　A　B

(b)

Fig. 1. Partial representation of the structure of Fe$_2$Al$_3$Si$_3$. Projection on (010). (a) The basic unit: four polyhedra centred on Fe atoms at $y \simeq 1/8$. Large filled circles (and large numbers) represent Fe atoms, smaller open circles represent Al and smaller filled circles Si. (b) Infinite strips running parallel to [100], formed by basic units sharing Al(1)–Al(2) edges. The Fe atoms are numbered. Strips with Fe atoms at $y \simeq 1/8$ and $y \simeq -1/8$ are represented in pale grey and dark grey, respectively. The rest of the structure is generated by a 2$_1$ symmetry operation.

Table 1. *Fractional atomic coordinates and equivalent isotropic displacement parameters* (Å^2)

$$B_{eq} = (8\pi^2/3)\Sigma_i\Sigma_j U_{ij}a_i^* a_j^* \mathbf{a}_i.\mathbf{a}_j.$$

	x	y	z	B_{eq}
Fe(1)	0.55644 (6)	0.11825 (7)	0.72857 (3)	0.474 (6)
Fe(2)	0.55532 (6)	0.63784 (6)	0.73027 (3)	0.357 (7)
Fe(3)	0.75645 (6)	0.12979 (7)	0.46474 (3)	0.461 (7)
Fe(4)	0.76506 (6)	0.62166 (7)	0.46897 (3)	0.457 (6)
Si(1)	0.9089 (1)	0.1252 (2)	0.17331 (6)	0.62 (1)
Si(2)	0.9694 (1)	0.6229 (1)	0.15226 (6)	0.54 (1)
Si(3)	0.7919 (1)	0.1445 (1)	0.62357 (6)	0.66 (1)
Si(4)	0.7943 (1)	0.6138 (2)	0.62604 (6)	0.88 (1)
Si(5)	0.3994 (1)	0.1281 (1)	0.01080 (6)	0.57 (1)
Si(6)	0.3967 (1)	0.6210 (2)	0.03280 (6)	0.81 (1)
Al(1)	0.1762 (2)	0.0470 (1)	0.66762 (7)	0.98 (2)
Al(2)	0.1882 (2)	0.7039 (1)	0.67718 (7)	0.86 (2)
Al(3)	0.4502 (1)	0.1402 (1)	0.55058 (6)	0.47 (2)
Al(4)	0.4548 (1)	0.6175 (2)	0.55607 (6)	0.74 (1)
Al(5)	0.5521 (1)	0.1240 (2)	0.17459 (6)	0.59 (1)
Al(6)	0.2959 (1)	0.6231 (2)	0.22522 (7)	1.08 (2)

Table 2. *Selected geometric parameters* (Å, °)

Fe environment

Fe(1)—Fe(2^i)	2.8161 (6)	Fe(3)—Si(2^{xi})	2.2649 (9)
Fe(1)—Si(1^{ii})	2.498 (1)	Fe(3)—Si(3)	2.296 (1)
Fe(1)—Si(2^{ii})	2.361 (1)	Fe(3)—Si(5^{vi})	2.344 (1)
Fe(1)—Si(3)	2.356 (1)	Fe(3)—Si(6^{vi})	2.498 (1)
Fe(1)—Si(4^i)	2.2950 (9)	Fe(3)—Si(6^{xi})	2.489 (1)
Fe(1)—Al(1)	2.875 (1)	Fe(3)—Al(1^{iv})	2.490 (1)
Fe(1)—Al(2^{iii})	2.403 (1)	Fe(3)—Al(2^v)	2.531 (1)
Fe(1)—Al(3)	2.641 (1)	Fe(3)—Al(3)	2.597 (1)
Fe(1)—Al(5^{iv})	2.609 (1)	Fe(3)—Al(3^{iv})	2.701 (1)
Fe(1)—Al(6^v)	2.479 (1)	Fe(3)—Al(4^v)	2.606 (1)
Fe(1)—Al(6^{vi})	2.652 (1)		
Fe(2)—Fe(1^{vii})	2.8161 (6)	Fe(4)—Si(1^{xii})	2.3346 (9)
Fe(2)—Si(1^{ii})	2.549 (1)	Fe(4)—Si(4)	2.2672 (9)
Fe(2)—Si(2^{viii})	2.357 (1)	Fe(4)—Si(5^{vi})	2.361 (1)
Fe(2)—Si(3^{vii})	2.316 (1)	Fe(4)—Si(5^{xii})	2.4082 (9)
Fe(2)—Si(4)	2.366 (1)	Fe(4)—Si(6^x)	2.500 (1)
Fe(2)—Al(1^{ix})	2.417 (1)	Fe(4)—Al(3^v)	2.523 (1)
Fe(2)—Al(2)	2.752 (1)	Fe(4)—Al(4)	2.631 (1)
Fe(2)—Al(4)	2.579 (1)	Fe(4)—Al(4^v)	2.557 (1)
Fe(2)—Al(5^v)	2.567 (1)	Fe(4)—Al(5^{xii})	2.528 (1)
Fe(2)—Al(6^v)	2.493 (1)		
Fe(2)—Al(6^x)	2.645 (1)		

Si(3)–Al(6)–Si(4)–Al(6) common face to Fe(1) and Fe(2) polyhedra

Si(3)—Al(6^v)	3.021 (2)	Al(6^v)—Si(3)—Al(6^{vi})	97.75 (4)
Si(3)—Al(6^{vi})	2.674 (2)	Al(6^v)—Si(4)—Al(6^x)	98.81 (4)
Si(4)—Al(6^v)	3.024 (2)	Si(3^v)—Al(6)—Si(4^v)	80.87 (4)
Si(4)—Al(6^x)	2.624 (2)	Si(3^v)—Al(6)—Si(4^{xiii})	82.14 (5)

Si and Al environments: (a) total number of neighbouring atoms at a distance less then 3.1 Å; (b) number of neighbouring Fe atoms; (c) Si—Fe or Al—Fe average distance.

	(a)	(b)	(c)		(a)	(b)	(c)
Si(1)	9	3	2.460 (1)	Al(1)	12	3	2.594 (1)
Si(2)	10	3	2.328 (1)	Al(2)	12	3	2.562 (1)
Si(3)	10	3	2.323 (1)	Al(3)	12	4	2.615 (1)
Si(4)	11	3	2.309 (1)	Al(4)	11	4	2.593 (1)
Si(5)	11	3	2.371 (1)	Al(5)	12	3	2.568 (1)
Si(6)	11	3	2.496 (1)	Al(6)	12	4	2.567 (1)

Symmetry codes: (i) $\frac{3}{2} - x, y - \frac{1}{2}, \frac{3}{2} - z$; (ii) $x - \frac{1}{2}, \frac{1}{2} - y, \frac{1}{2} + z$; (iii) $\frac{1}{2} - x, y - \frac{1}{2}, \frac{3}{2} - z$; (iv) $1 - x, -y, 1 - z$; (v) $1 - x, 1 - y, 1 - z$; (vi) $\frac{1}{2} + x, \frac{1}{2} - y, \frac{1}{2} + z$; (vii) $\frac{3}{2} - x, \frac{1}{2} + y, \frac{3}{2} - z$; (viii) $x - \frac{1}{2}, \frac{3}{2} - y, \frac{1}{2} + z$; (ix) $\frac{1}{2} - x, \frac{1}{2} + y, \frac{3}{2} - z$; (x) $\frac{1}{2} + x, \frac{3}{2} - y, \frac{1}{2} + z$; (xi) $\frac{3}{2} - x, y - \frac{1}{2}, \frac{1}{2} - z$; (xii) $\frac{3}{2} - x, \frac{1}{2} + y, \frac{1}{2} - z$; (xiii) $x - \frac{1}{2}, \frac{3}{2} - y, z - \frac{1}{2}$.

the other Si—Fe distances, suggest that Si(1) and Si(6) could be mixed (Si,Al) sites. However, no significant decrease in the *R* factor was observed by varying the occupancies of these sites to fit the experimental formula Fe$_2$Al$_{3.2}$Si$_{2.8}$.

It is noteworthy that all the atoms in the structure, except Al(1) and Al(2), have a *y* coordinate close to 1/8, 3/8, 5/8 and 7/8. In addition, as Table 1 clearly shows, for each atom of coordinates *x*, *y*, *z* there is a non-equivalent atom of the same element with coordinates $x' \simeq x$, $y' \simeq y+1/2$, $z' \simeq z$. [Only two pairs, Al(1)–Al(2) and Al(5)–Al(6), do not verify all these relations.] As a result, the structure can be considered to be a superstructure of a hypothetical simpler one with unit cell $a' = a$, $b' = b/2$, $c' = c$ and space group *I2/m*. This pseudosymmetry is responsible for the low intensities observed for two categories of *hkl* reflections: $k = 2n + 1$ and $h + 1/2k + l = 2n + 1$.

Table 3. Faces (F), edges (E) and corners (C) shared by Fe polyhedra

Each polyhedron is designated by its Fe central atom followed by a letter indicating the Fe y coordinate: a, b, c, b', c' for $y \simeq \frac{1}{8}, \frac{3}{8}, \frac{5}{8}, -\frac{1}{8}$ and $-\frac{3}{8}$, respectively. Polyhedra lying at $y \simeq \frac{1}{8}$ are taken as the reference.

	[Fe1] a	[Fe2] a	[Fe3] a	[Fe4] a
[Fe1] a	–	F Al(6)-Si(3)-Al(6)-Si(4) / E Al(1)-Al(2)	E Al(3)-Si(3)	C Si(4)
[Fe2] a	F Al(6)-Si(3)-Al(6)-Si(4) / E Al(1)-Al(2)	–	C Si(3)	E Al(4)-Si(4)
[Fe3] a	E Al(3)-Si(3)	C Si(3)	–	–
[Fe4] a	C Si(4)	E Al(4)-Si(4)	–	–
[Fe1] b	–	–	C Al(2)	E Si(1)-Al(3)
[Fe2] b	–	–	F Al(2)-Al(4)-Si(2)	C Al(5)
[Fe3] b	C Al(2)	F Al(2)-Al(4)-Si(2)	–	E Al(4)-Al(3) / E Si(6)-Si(5)
[Fe4] b	E Si(1)-Al(3)	C Al(5)	E Al(4)-Al(3) / E Si(6)-Si(5)	–
[Fe1] b'	–	–	E Al(1)-Al(3)-Si(2)	C Al(5)
[Fe2] b'	–	–	C Al(1)	E Al(4)-Si(1)
[Fe3] b'	F Al(1)-Al(3)-Si(2)	C Al(1)	E Si(6)-Si(6) / E Al(3)-Al(3)	–
[Fe4] b'	C Al(5)	E Al(4)-Si(1)	–	E Al(4)-Al(4) / E Si(5)-Si(5)
[Fe1] c	C Al(6)	F Al(6)-Al(5)-Si(2)	–	–
[Fe2] c	E Al(6)-Si(1)	C Al(6)	–	–
[Fe3] c	–	–	–	E Si(6)-Al(3)
[Fe4] c	–	–	E Al(4)-Si(5)	–
[Fe1] c'	C Al(6)	E Al(6)-Si(1)	–	–
[Fe2] c'	F Al(6)-Al(5)-Si(2)	C Al(6)	–	–
[Fe3] c'	–	–	–	E Al(4)-Si(5)
[Fe4] c'	–	–	E Si(6)-Al(3)	–

Experimental

The phase was elaborated at the Laboratoire Central de Recherche de Chedde of the Péchiney Electrométallurgie Society. A mixture of the pure elements in atomic proportions Fe:Al:Si of 5:8:7 was melted at 1373 K for 2 h, then annealed at 1073 K for 64 h, and finally furnace-cooled to room temperature. Small single crystals were obtained by grinding the ingot.

Crystal data

$Fe_2Al_3Si_3$
$M_r = 276.9$
Monoclinic
$P2_1/n$
$a = 7.179\,(2)$ Å
$b = 8.354\,(2)$ Å
$c = 14.455\,(4)$ Å
$\beta = 93.80\,(2)°$
$V = 865.1\,(7)$ Å^3
$Z = 8$
$D_x = 4.25$ Mg m^{-3}

Mo $K\alpha$ radiation
$\lambda = 0.71073$ Å
Cell parameters from 25 reflections
$\theta = 8.28–24.10°$
$\mu = 7.91$ mm^{-1}
$T = 294$ K
Roughly prismatic, elongated along [$\bar{1}01$]
$0.18 \times 0.07 \times 0.05$ mm
Grey with metallic shine

Data collection

Enraf–Nonius CAD-4 diffractometer
$\theta/2\theta$ scans
Absorption correction:
by integration from crystal shape (ABSCOR; Coppens, Leiserowitz & Rabinovich, 1965)
$T_{min} = 0.63$, $T_{max} = 0.70$
4864 measured reflections
2517 independent reflections

1289 observed reflections
$[I > 3\sigma(I)]$
$R_{int} = 0.031$
$\theta_{max} = 30°$
$h = -10 \rightarrow 10$
$k = 0 \rightarrow 11$
$l = -20 \rightarrow 20$
3 standard reflections
frequency: 120 min
intensity decay: 4.7% (corrected)

Refinement

Refinement on F
$R = 0.0170$
$wR = 0.0218$
$S = 0.64$
1289 reflections
146 parameters
$w = 1/\sigma^2(F)$
$(\Delta/\sigma)_{max} = 0.01$

$\Delta\rho_{max} = 0.5\,(2)$ e Å^{-3}
$\Delta\rho_{min} = -0.6\,(2)$ e Å^{-3}
Extinction correction: Stout & Jensen (1968)
Extinction coefficient: $2.40\,(8) \times 10^{-7}$
Atomic scattering factors from International Tables for X-ray Crystallography (1974, Vol. IV)

As in $FeAl_3Si_2$, aluminium and silicon were difficult to distinguish. The distribution finally retained for the Al and Si atoms on the M sites corresponds to that resulting in the lowest R factor. But more significantly, (i) this distribution leads to, for every Al atom, an Al—Fe average distance greater than the average Si—Fe distance (see Table 2), and (ii) it is in good agreement with the I2/m pseudosymmetry of the structure.

The crystal structure was solved by direct methods using the program MULTAN11/82 (Main, Fiske, Hull, Lessinger, Germain, Declercq & Woolfson, 1982). All programs used belong to the SDP system (B. A. Frenz & Associates Inc., 1982).

References

Anglézio, J. C. (1990). PhD thesis, Univ. of Paris-Sud, Orsay, France.

B. A. Frenz & Associates Inc. (1982). *SDP Structure Determination Package*. College Station, Texas, USA.

Coppens, P., Leiserowitz, L. & Rabinovich, D. (1965). *Acta Cryst.* **18**, 1035–1038.

Guéneau, C. (1993). PhD thesis, Univ. of Paris-Sud, Orsay, France.

Guéneau, C., Servant, C., d'Yvoire, F. & Rodier, N. (1995). *Acta Cryst.* **C51**, 177–179.

Main, P., Fiske, S. J., Hull, S. E., Lessinger, L., Germain, G., Declercq, J.-P. & Woolfson, M. M. (1982). *MULTAN11/82. A System of Computer Programs for the Automatic Solution of Crystal Structures from X-ray Diffraction Data*. Univs. of York, England, and Louvain, Belgium.

Stout, G. H. & Jensen, L. H. (1968). In *X-ray Structure Determination*. London: MacMillan.

Zarechnyuk, O. S., German, N. V., Yanson, T. I., Rykhal, R. M. & Muraveva, A. A. (1981). *Fazouye Ravnovesiya, met. Splavakh*, pp. 69–73.

Rhombohedral Ce₂Ni₅Zn₂ and Hexagonal CeNi₂Zn: the First Ternary Compounds from the Ce–Ni–Zn System

VOLODYMYR VASYL'OVYCH PAVLYUK, IGOR MYCHAJLOVYCH OPAINYCH AND OKSANA IVANIVNA BODAK

Department of Inorganic Chemistry, L'viv University, 6 Lomonosova Street, 290005 L'viv 5, Ukraine

RADOVAN ČERNÝ AND KLAUS YVON

Laboratoire de Cristallographie, Université de Genève, 24 quai Ernest-Ansermet, CH-1211 Geneva 4, Switzerland

(*Received 13 February 1995; accepted 17 May 1995*)

Abstract

Dicerium pentanickel dizinc, Ce₂Ni₅Zn₂, crystallizes as a new ordered substitution variant of the Er₂Co₇ structure type. Cerium dinickel zinc, CeNi₂Zn, crystallizes with the YRh₂Si structure type. Both structures contain MgZn₂- and CaCu₅-type slabs which occur in ratios of 1:2 in Ce₂Ni₅Zn₂ and 1:1 in CeNi₂Zn.

Comment

No ternary phases have been reported in R–Ni–Zn systems (where R is a rare earth element). Our investigations of the phase equilibria in the Ni-rich region of the Ce–Ni–Zn system at 470 K have revealed the following compounds: rhombohedral Ce₂Ni₅Zn₂ form-

ing with the nominal compositions Ce₂₅Ni₅₅Zn₂₀ and Ce₂₂.₅Ni₅₅Zn₂₂.₅, and hexagonal CeNi₂Zn forming with the nominal compositions Ce₂₅Ni₃₅Zn₄₀, Ce₂₅Ni₄₀Zn₃₅, Ce₂₅Ni₅₀Zn₂₅ and Ce₂₂Ni₅₀Zn₂₈

Ce₂Ni₅Zn₂ crystallizes as an ordered substitution variant of the Gd₂Co₇ structure type (Bertaut, Lemaire & Schweizer, 1965), also known as the Er₂Co₇ structure type (Ostertag, 1967). Ni and Zn occupy the Co positions 6(c) and 18(h), and 3(b) and 9(e), respectively, in space group $R\bar{3}m$. Another ordered substitution variant of this structure type is Y₄Rh₉Si₅ (Paccard, Paccard, Moreau & Gomez Sal, 1985), in which Rh and Si occupy the positions 9(e) and 18(h), and 3(b) and 6(c), respectively.

The distribution of Ni and Zn in the structure of Ce₂Ni₅Zn₂ could not be determined from X-ray data alone because of a lack of scattering contrast. The following two arguments support the proposed distribution. Firstly, the composition of the model is close to the nominal compositions of the alloys for which crystals of Ce₂Ni₅Zn₂ were found. A model with Y₄Rh₉Si₅-type distribution would correspond to the nominal compositions of the alloys for which crystals of CeNi₂Zn were found. Secondly, the bond distances associated with the positions 3(b) and 9(e) are longer than those associated with the 6(c) and 18(h) positions. This is in accordance with the larger atomic radius of Zn compared to that of Ni. As shown in Fig. 1, the structure contains the following coordination polyhedra: Ce1 [Ni₁₂Zn₆Ce₂], Ce2 [Ni₉Zn₃Ce₄], Ni1 [Ni₆ZnCe₅], Ni2 and Ni3 [Ni₆Zn₃Ce₃], Zn1 [Ni₄Zn₄Ce₄], Zn2 [Ni₆Ce₆].
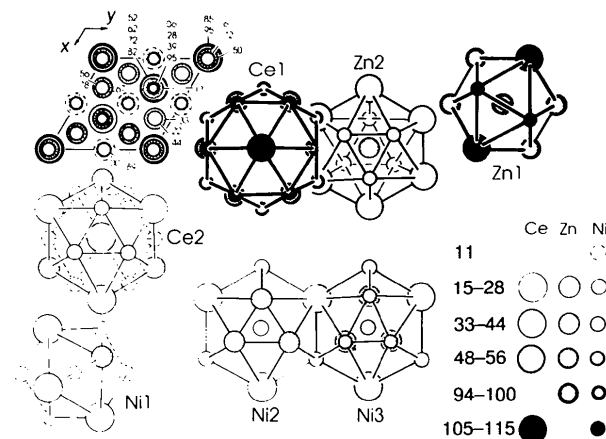

Fig. 1. Structural projection of rhombohedral Ce₂Ni₅Zn₂ along [001] showing the coordination polyhedra.

CeNi₂Zn crystallizes with the YRh₂Si structure type (Paccard & Paccard, 1985), which is an ordered substitution variant of the CeNi₃ structure type (Cromer & Olsen, 1959). Its structural projection is shown in Fig. 2. The structure contains the following coordina-